ARE WATER-EQUIVALENT MATERIALS USED IN ELECTRON BEAMS DOSIMETRY REALLY WATER EQUIVALENT?

C. BORCIA, D. MIHAILESCU

Faculty of Physics, "Al. I. Cuza" University, Iasi, e-mail: dmihail@uaic.ro

Received May 14, 2007

In order to analyse the degree to which water-equivalent materials are water equivalent, we investigate here not only the depth dose distributions, but also the energy distributions and angular spread of electrons in water and some commercially available water substitute solid phantoms. Accurate simulations using EGSnrc and DOSXYZnrc Monte Carlo codes were done for pencil and 10×10 cm^2 parallel beams perpendicularly incident on water and solid phantoms (polystyrene, PMMA and solid water WT1). Monoenergetic beams of 6, 9, 12, 15 and 18 MeV were used.

Key words: dosimetry, electron beams, plastic phantoms, IAEA TRS-398.

1. INTRODUCTION

The condition for two phantom materials to be considered as *exactly equivalent* is that the following three physical quantities are identical for the whole electron range under consideration: linear collision stopping power (S_{col}), linear radiative stopping power (S_{rad}) and linear scattering power (T) [1]. These quantities influence the energy and angular distributions of electrons inside the phantom and, consequently, the depth dose distributions. All these distributions (energy, angular and dose deposition) should be theoretically identical, at any depth in a water-equivalent material phantom, with those obtained in a water phantom at the same depth. For dosimetry purposes, dose deposition distributions are the most important.

There is a lot of data in the literature (measurements and simulations) which demonstrate that there is no perfect match between depth dose distributions for any water substitute material [2–14]. However, there are some plastics, referred as water-equivalent materials (see Table 1) used as water substitute for dosimetry purposes in radiotherapy and radiophysics departments. In this case it is necessary to scale depths measured in non-water phantoms to water equivalent depths. In addition, the reading of an ionization chamber in the non-water phantom must be converted to an appropriate reading in water. As we shown elsewhere [13], applying the IAEA recommended scaling procedure [15] for polystyrene, PMMA and Solid water WT1, the discrepancies between depth-

dose curves in water and the scaled depth-dose curves in these plastic materials became negligible. This result could signify that electron energy and angular distributions in water at a given depth should be the same with those in plastic phantoms at scaled depths, but this still remains to be proved. It is the goal of this work to confirm or not this assumption. According to Ding *et al.* [12], there is another scaling of depths which causes the mean energies of electrons to be the same at corresponding depths and, by supposition, also the electron spectra to be identical. Nonetheless, due to the differences in scattering and stopping-powers of different materials, there is still an overall difference in the absolute magnitude of the electron fluence.

2. THEORETICAL

In various radiation dosimetry protocols [15–18] plastic is allowed in addition to water as a phantom material for determination of absorbed dose to water in radiotherapy electron beams. According to the IAEA International Code of Practice TRS-398 [15], solid phantoms in slab form such as polystyrene, PMMA, and certain epoxy resin "solid water" (water substitute) phantom materials such as solid water, plastic water, virtual water, etc. (see Table 1) may be used for low energy electron beam dosimetry (under 10 MeV) and are generally required

Table 1

Elemental composition (fraction by weight), nominal density and mean atomic number of common phantom materials used as water substitutes (for comparison, liquid water is also included) [15]

	Liquid water[a]	**Solid water WT1[a]**	**Solid water RMI-457**	**Plastic water**	**Virtual water**	**PMMA[a,b]**	**Polystyrene[a]**
H	0.1119	0.0810	0.0809	0.0925	0.0770	0.0805	0.0774
C		0.6720	0.6722	0.6282	0.6874	0.5998	0.9226
N		0.0240	0.0240	0.0100	0.0227		
O	0.8881	0.1990	0.1984	0.1794	0.1886	0.3196	
F							
Cl		0.0010	0.0013	0.0096	0.0013		
Ca		0.0230	0.0232	0.0795	0.0231		
Br				0.0003			
ρ [g/cm^3]	1.000	1.020	1.030	1.013	1.030	1.19	1.060
$\bar{Z}^c$	6.6	5.95	5.96	6.62	5.97	5.85	5.29

[a] See Refs. [19, 20].

[b] Polymethyl methacrylate, also known as acrylic. Trade names are Lucite, Plexiglas or Perspex.

[c] For the definition of mean atomic number see, for instance, Ref. [1].

for low energy X rays. Nevertheless, the dose determination must always be referred to the absorbed dose to water at the reference depth in a homogeneous water phantom. Ideally, the phantom material should be water equivalent; that is, it should have the same absorption and scatter properties as water.

Depth dose distributions in plastic phantoms can be converted to appropriate depth dose distribution in water by means of depth-scaling. For a measurement made at a depth z_{pl} ($g \cdot cm^{-2}$) in a plastic phantom, the appropriate depth in water z_w ($g \cdot cm^{-2}$) is given by:

$$z_w = z_{pl}\, c_{pl} \tag{1}$$

in which c_{pl} is the fluence-scaling factor. When $M_{Q,\,pl}$ is the reading of an ionization chamber at $z_{ref,\,pl}$ in the solid phantom and M_Q is the reading at z_{ref} in water, h_{pl} is defined as

$$h_{pl} = \frac{M_Q}{M_{Q,pl}}\,. \tag{2}$$

In the case of identical irradiation condition, when the absorbed dose to water is D_w and the absorbed dose to solid phantom is D_{pl}, the fluence-scaling factor can be calculated [5, 13] as:

$$h_{pl} = \frac{M_Q}{M_{Q,\,pl}} = \frac{D_w}{D_{pl}} s_{pl,w} \tag{3}$$

where $s_{pl,\,w}$ is the plastic material-to-water stopping power ratio.

The IAEA recommended values for the depth-scaling factors c_{pl} and fluence-scaling factors h_{pl} are given in Table 2 [15].

Table 2

Values for the depth-scaling factor c_{pl}, the fluence scaling factor h_{pl} and the nominal density ρ_{pl} for certain plastics [15]

Plastic phantom	c_{pl}	h_{pl}	ρ_{pl}
Solid water (WT1)	0.949	1.011	1.020
Solid water (RMI-457)	0.949	1.008[a]	1.030
Plastic water	0.982	0.998[b]	1.013
Virtual water	0.946	---[c]	1.030
PMMA	0.941	1.009	1.190
Polystyrene	0.922	1.026	1.060

[a] Average of the values given in [8] under 10 MeV.
[b] Average of the values given in [14] under 10 MeV.
[c] Data not available.

When using a plastic phantom to determine the depth dose distribution, each measurement depth in plastic must be scaled using equation (1) to give the appropriate depth in water. The dosimeter reading at each depth must also be scaled using equation (2). If an ionization chamber is used, the measured depth ionization distribution must be converted to a depth dose distribution by multiplying the ionization current at each depth by the appropriate stopping-power ratio $s_{w,\,air}$.

3. MODELING

3.1. DEPTH DOSE DISTRIBUTIONS CALCULATIONS

In a previous paper [13], we have calculated the depth dose distributions for monoenergetic 6 to 18 MeV electron pencil beams and 10×10 cm^2 electron parallel beams normally incident on water and some plastic materials phantoms (polystyrene, PMMA and WT1). The absorbed dose distributions were calculated using DOSXYZnrc [21] and stopping power ratios (SPRs) with SPRRZnrc [22] Monte Carlo code. The fluence-scaling factors were determined using the relation (4).

The EGSnrc (Electron Gamma Shower) system [23] is a package for the Monte Carlo simulation of coupled electron-photon transport. DOSXYZnrc is an EGSnrc user code used to calculate dose in Cartesian voxels. SPRRZnrc is an extensively tested EGSnrc user code used to calculate Spencer-Attix stopping-power ratios for photon and electron beams in a cylindrical geometry. In our work, the SPRs have been calculated along the central axis of the electron beams in cylindrical regions with a thickness of 0.1 cm and a radius of 1 cm.

In all simulations, we have used default values for EGSnrc particle's transport parameters, PRESTA-I for boundary crossing algorithm and PRESTA-II as electron transport algorithm. The cross section data were created using PEGS4 [23] including Sternheimer density effect corrections from ICRU 37 [20]. The energy cut-offs for particle transport were set to ECUT = AE = 0,521 MeV (kinetic energy plus rest mass) and PCUT = AP = 0,010 MeV.

The geometry used for DOSXYZnrc calculation is shown in Fig. 1. A $10 \times 10 \times 5$ cm^3 phantom was used for 6 and 9 MeV, while for higher energies (12, 15 and 18 MeV) the phantom size was $10 \times 10 \times 10$ cm^3. In both cases, the dose distributions are calculated along the z-axis in 50 voxels.

For lower energies (6 and 9 MeV), the voxel dimensions (crossplane $\times$ $\times$ inplane depth) along the z-axis were settled to 1 cm $\times$ 1 cm $\times$ 0.1 cm, while for 12, 15 and 18 MeV electron beam energies, the bin dimensions were 1 cm $\times$ 1 cm $\times$ 0.2 cm. The number of source electrons was equal to 10^6 for pencil beams and 10×10^6 for 10×10 cm^2 for parallel beams. By using this number of histories the average dose uncertainty in each voxel was less than 1.0%.

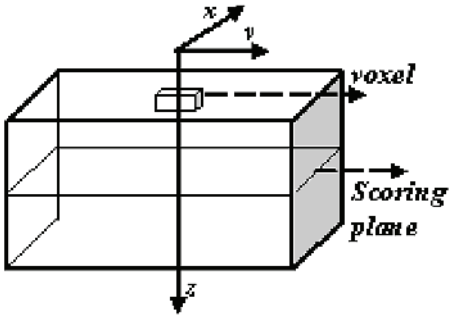

Fig. 1 – Geometry used to calculate dose distributions with DOSXYZnrc.

3.2. ENERGY AND ANGULAR DISTRIBUTIONS CALCULATIONS

In order to calculate the energy and angular distributions at different depths z in a phantom, a two steps procedure has been employed. The first step consists of scoring the data about each electron crossing the plane situated at a given depth z in phantom. In the second step, data previously obtained is analysed. We have simulated the passing of electron beams through the water or plastic phantom using BEAMnrc [24] code, a scoring plane being placed at the appropriate depth z (see Fig. 1). The outputs phase-space data for every depth have been analysed with BEAMDP code [25].

BEAMnrc [24] is an EGSnrc [23] based general purpose Monte Carlo code originally developed for simulating radiotherapy beams from accelerators or ^{60}Co units. BEAMnrc models the therapy source with the z-axis taken as the beam-axis. The model consists of a series of component modules (CMs), each of which is contained between two planes which are perpendicular to the z-axis. There can be an arbitrary number of scoring planes which are at the back plane of a CM and thus perpendicular to the z-axis. The main output of BEAMnrc is a phase-space data file for every scoring plane. The phase-space files contain all the information about every particle that cross the appropriate scoring plane, *i.e.* charge (electron, photon or positron), energy, moving direction, and the entire history of that particle. The particle history is scored trough a special 28 bit variable named LATCH [21, 24]. The LATCH technique allows one, for instance, to separate the effects of primary and secondary electrons, or identify those particles that have passed or interacted in certain components of the simulated system (accelerator, ^{60}Co machine or phantom).

BEAMDP (BEAM Data Processor) [25] was developed to help the BEAMnrc [24] users to analyze the electron beam data obtained by the Monte Carlo simulation of the coupled transport of photons and electrons in different simulated systems. In addition to energy and angular distributions, BEAMDP can be used to determine many other beam characteristics such as fluence *vs.* position, energy-fluence *vs.* position, energy-fluence distributions, mean energy

distributions, etc. Full documentation (manuals and papers) can be found on the web site of The National Research Council of Canada (http://www.irs.inms.nrc.ca).

The phantom models used for BEAMnrc calculations were the same described in section 3.1 (Fig. 1). A scoring plane was placed at a chosen depth z. Most of our calculations have been done at the reference depth, z_{ref}. The value of z_{ref} will be defined later in this paper. The electron planar fluence has been scored only in the central region of the phantom, in rectangular bins centred on z-axis and having the same crossplane × inplane dimensions (1 cm × 1 cm) like those used for dose distribution calculations. In order to calculate the energy spectra of simulated beams at a given scoring plane the particles fluence (planar or actual) [25] is scored in a user-specified field *vs.* particles energy with energy bins of equal bin width within a specified spatial region. Fluence is normalized to the bin width and the number of incident particles. The angular distributions are calculated as the total number of particles scored in an angular bin of equal bin width within a specified spatial region.

4. RESULTS AND DISCUSSION

4.1. DEPTH DOSE DISTRIBUTIONS

Comparison of depth dose distributions function of electron energy, media and beam size are shown in Fig. 2a, b and c, respectively. Each distribution is normalized to the maximum dose value. The necessity of depth scaling is illustrated by Fig. 2b, while the significant differences between dose distributions obtained with pencil and 10 × 10 cm^2 parallel beams are shown in Fig. 2c. When a phantom is irradiated with a narrow beam of electrons, most of the electrons are scattered out of the narrow beam and the dose decreases rapidly with depth. When the field size is increased, this loss of electrons on the central axis is compensated by the electrons scattered from the edges of the irradiated volume towards the central axis, and the depth dose increases gradually with field size as long as the distance between the point of measurement and the edge of the field is shorter than the maximum range of the electrons. For larger field sizes, the central axis depth dose is independent of field size.

4.2. WATER EQUIVALENCY

Depth-scaling factors, c_{pl}, have been previously calculated [13] as:

$$c_{pl} = \frac{z_{av}^{w} \rho_{w}}{z_{av}^{pl} \rho_{pl}} \tag{4}$$

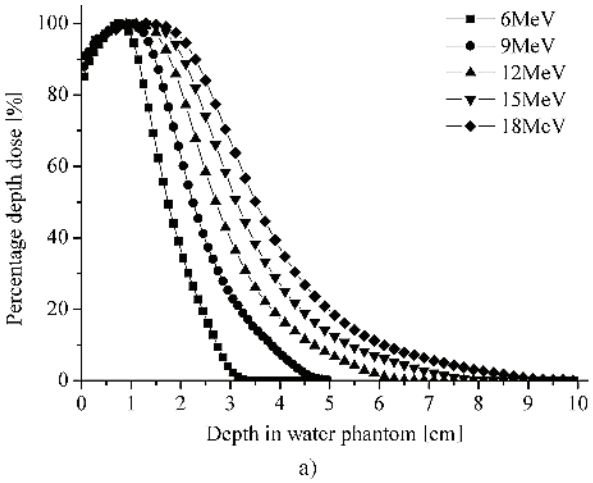

a)

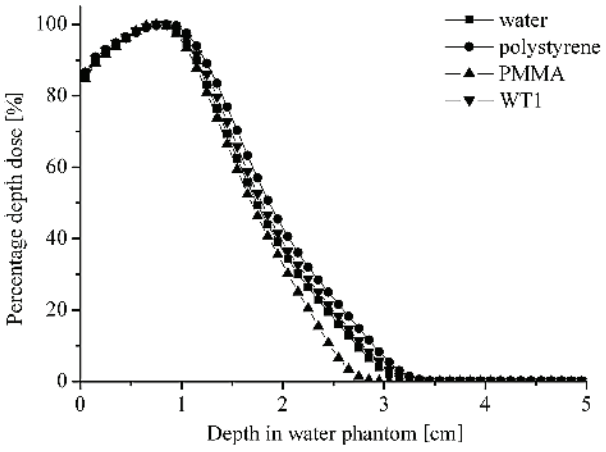

b)

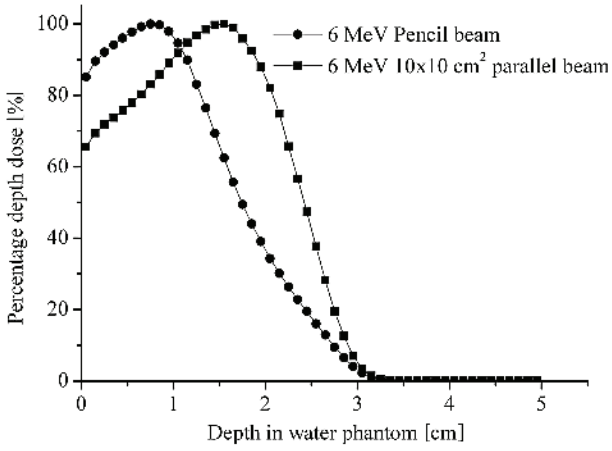

c)

Fig. 2 – Absorbed depth dose in water phantom: (a) different energies; (b) different media, (c) different beam sizes.

where z_{av}^{w} and z_{av}^{pl} is an average penetration depth (cm) in water and solid phantom, and ρ_w and ρ_{pl} is the density (g·cm^{-3}) of water and solid phantom material, respectively. The penetration depths z_i of each history were sampled and z_{av} was calculated using EGSnrc Monte Carlo code. For 10×10 cm^2 parallel mono-energetic electron beams, and generally good agreement with TRS-389 values was obtained (see Table 3). The c_{pl} values for pencil beams have been found to be generally lower (up to 10%) than the reference (10×10 cm^2) beam values. However, only the c_{pl}s calculated for the reference beams can be compared with those recommended by TRS-398, and only for beam qualities $R_{50} < 4$ g/cm^2 ($E_0 < 10$ MeV).

Table 3

Monte Carlo calculated mean scaling-factors [13]. For every material, two different values are given. First row stands for pencil beams, while the second has been obtained for 10×10 cm^2 parallel beams. The values from parenthesis indicate the relative differences to the TRS-398 recommended values

Plastic phantom	c_{pl}	h_{pl}
Polystyrene	0.883	1.018
	0.930 (+0.9%)	1.037 (+1.1%)
PMMA	0.878	1.013
	0.945 (+0.4%)	1.018 (+0.9%)
WT1	0.954	1.011
	0.952 (+0.3%)	1.019 (+0.8%)

We have evaluated the percentage depth dose distributions in solid phantoms with and without scaling for pencil and 10×10 cm^2 parallel beams. Good agreements between dose distributions in water and those obtained by IAEA scaling method using c_{pl} factors have been obtained for both pencil and 10×10 cm^2 electron beams, although in the last case we observed some minor differences near the surface and at the end of the electron range (see, for instance, Figs. 3 and 4).

Some authors [11] use the water equivalent thickness of 1 mm plastic to describe the water equivalence of water-substitute materials. Using the equation (1), we obtain:

$$z_w(\text{mm}) = \frac{\rho_{pl} \cdot c_{pl}}{\rho_w} \cdot z_{pl}(\text{mm}) = \frac{\rho_{pl} \cdot c_{pl}}{\rho_w} \tag{5}$$

the results for non-water materials analysed by us being tabulated below.

There are significant differences between plastic materials investigated in this paper. Excepting the PMMA case, 1 mm plastic is equivalent with less than

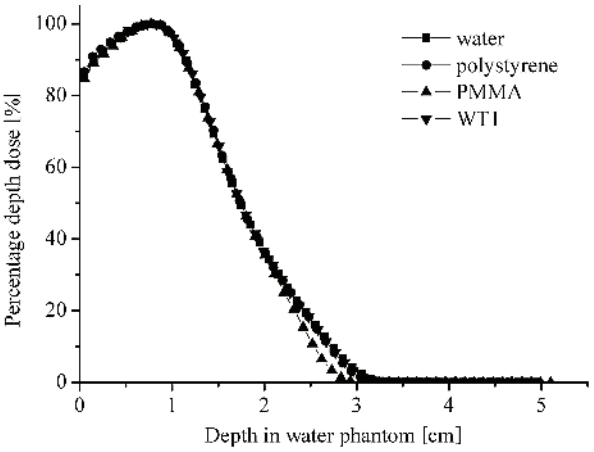

Fig. 3 – Depth dose distributions from Fig. 2(b) after scaling using c_{pl} factors (Table 3) for a 6 MeV pencil beam.

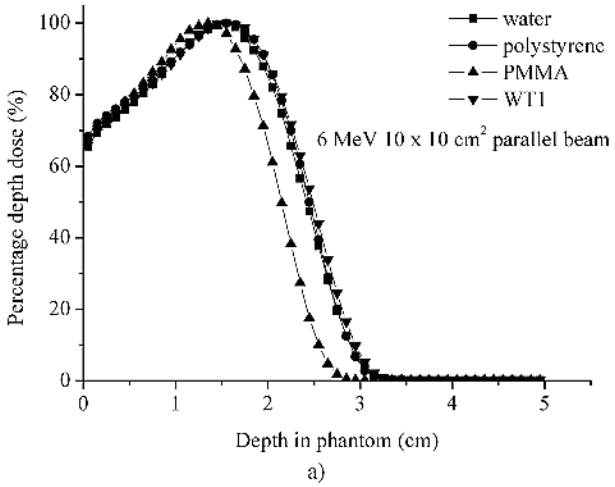

a)

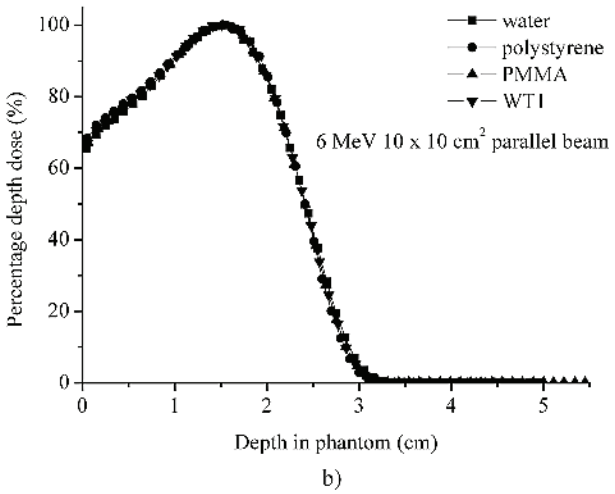

b)

Fig. 4 – Comparison of depth dose distributions obtained in water and water-equivalent phantoms without (a) and with c_{pl} correction (b) in the case of 6 MeV, 10 × 10 cm^2 parallel beam.

1 mm water, fact illustrated by the depth dose distribution curves for these materials which are situated on the right side of the corresponding curve of water, when the irradiation conditions are the same. Due to the much higher mass density, PMMA reveal an opposite behaviour, the depth dose distributions curves being situated in this case on the left side of the water curve. This general behaviour of depth dose distributions curves has been found to be independent of the beam quality (see the Figs. 2b and 4a).

If we consider the values from Table 4 as indicators of water-equivalency, then WT1 has the best equivalency. WT1 is an epoxy resin ("solid water") material like plastic water or virtual water (see Tables 1 and 2). There is a new epoxy resin phantom material, named WTe, which has even better characteristics than WT1. McEwen and DuSautoy [11] have found 1 mm WTe = 1.01 mm water. Note that the above considerations do not take into consideration the fluence-scaling factors, which also have different values for different plastic materials.

The use of epoxy resin phantoms offers a number of advantages over water for radiotherapy dosimetry in terms of robustness and ease of use. In addition, these plastic water substitutes do not exhibit charge stored effects like PMMA does.

Table 4

Water-equivalency for plastic materials investigated in this work, expressed in water equivalent thickness of 1cm plastic (1 mm plastic = *n* mm water, with *n* given by the following values)

Plastic phantom	**Pencil beam**	**10 × 10 cm²**
Polystyrene	0.936	0.986
PMMA	1.045	1.125
WT1	0.973	0.971

4.3. ENERGY DISTRIBUTIONS AND ANGULAR SPREADS

The energy and angular distributions for different beams quality at the reference depth z_{ref} in water and at the corresponding scaled depth:

$$z_{pl}(\mathrm{cm}) = \frac{\rho_w}{\rho_{pl} \cdot c_{pl}} \cdot z_{ref,\,w}(\mathrm{cm}) \tag{6}$$

in non-water phantoms have been calculated. The reference depths were determined with [1]:

$$z_{ref} = 0.6R_{50} - 0.1, \tag{7}$$

where R_{50} is the half-value depth, *i.e.* the depth in phantom at which the percentage depth dose became 50% of dose maximum. The purpose of these calculations was to verify if the energy spectra and angular distributions at a

given depth in water and at corresponding scaled depth in plastic phantoms are the same. In Fig. 5 are shown the distributions obtained for a 6 MeV pencil beam perpendicularly incident on phantom. The bin size of spectra and angular distributions is 30 KeV and 1°, respectively. The electron planar fluence and the number of electrons is normalized to the bin width and the number of incident electrons (10^6, in this case). Similar distributions curves have been obtained for other beam qualities.

The distributions are not identical, mainly to the different number of particles arriving in the scoring plane (we remind the necessity of fluence-scaling, but is not clear if the same h_{pl} factors determined for dose distributions – see section 4.2 – can be used in the case of energy and angular distributions).

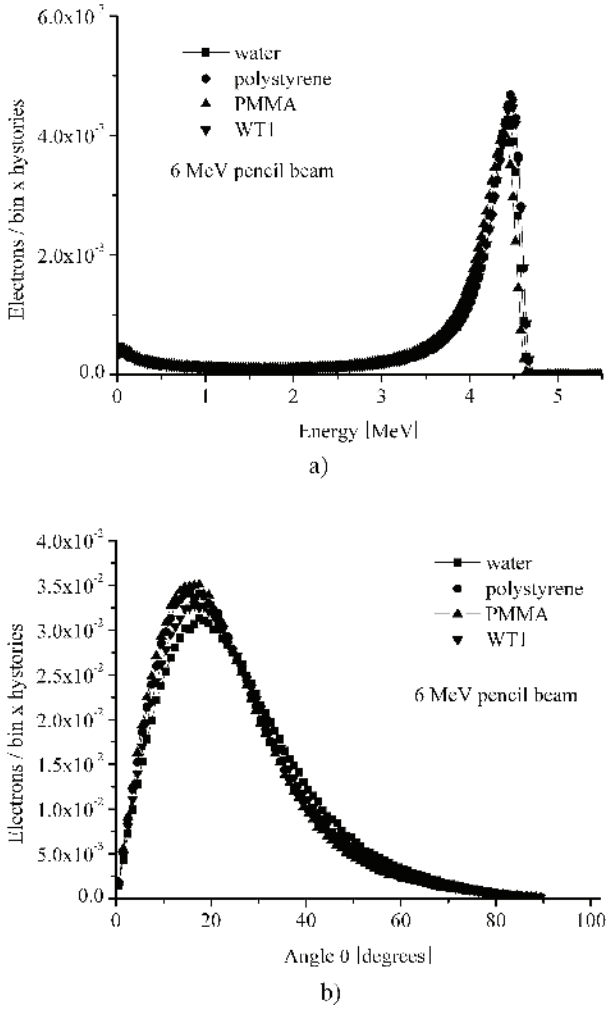

Fig. 5 – The energy spectra (a) and angular distributions (b) at the reference depth z_{ref} in water and at the corresponding scaled depths in non-water phantoms.

However, the mean energy $\bar{E}$ is independent of the number of scored electrons and should be the same after scaling, because the absorbed dose is the same. Surprisingly, our results do not confirm entirely the above supposition, significant differences between mean energies of electrons in water and plastic phantoms being obtained (see, for example, Table 5). The reason for such disagreement could be the way in which we have calculated these spectra, *i.e.* in a plane and not in a voxel.

Table 5

Energy parameters determined from electron spectral distributions obtained for a 6 MeV electron pencil beams normally incident on water and some plastic phantoms

Phantom (depth in phantom)	E_{max} **[MeV]**	E_p **[MeV]**	$\bar{E}$ **[MeV]**
Water ($z_{ref,\,w} = 0.94$ cm)	4.67	4.43	3.69
Polystyrene ($z = 1.068 \times z_{ref,\,w}$)	4.70 (+0.6%)	4.46 (+0.7%)	3.79 (+2.7%)
PMMA ($z = 0.957 \times z_{ref,\,w}$)	4.61 (–1.3%)	4.31 (–2.0%)	3.62 (–1.9%)
WT1 ($z = 1.028 \times z_{ref,\,w}$)	4.70 (+0.6%)	4.46 (+0.7%)	3.76 (+1.9%)

5. CONCLUSIONS

The water equivalency of polystyrene, PMMA and an epoxy resin plastic material (the "solid water" WT1) has been investigated by calculating the water equivalent thickness of 1 mm plastic. Previously Monte Carlo calculated values for depth-scaling factors c_{pl} were used. In addition, energy spectra and angular distributions of electrons at reference depth z_{ref} in water were calculated and compared with those determined at the corresponding scaled depth in non-water phantoms. Mono-energetic (6 to 18 MeV) pencil and 10×10 cm^2 electron beams, normally incident on a water or plastic phantom, have been used.

Significant differences between plastic materials investigated in this paper have been found. The best equivalency with water has been obtained for "solid water" WT1 phantom material, *i.e.* 1 mm WT1 = 0.973 mm water (pencil beam) and 1 mm WT1 = 0.971 mm water (10×10 cm^2 parallel beam). Taking into account that epoxy resin phantoms offer some advantages over water, such as robustness, ease of use and no charge stored effects, we conclude that WT1 have better dosimetry characteristics than polystyrene or PMMA. However, the recommendation we made is to use a water phantom wherever possible.

REFERENCES

1. International Commission On Radiation Units And Measurements, *Radiation Dosimetry: Electron beams with energies between 1 and 50 MeV*, ICRU Report 35, Bethesda MD, 1984.
2. D. I. Thwaites, Phys. Med. Biol., **30**, 41 (1985).

3. I. A. D. Bruinvis, S. Heukelom, B. J. Mijnheer, Phys. Med. Biol., **30**, 1043 (1985).
4. V. M. Tello, R. C. Tailor, W. F. Hanson, Med. Phys., **22**, 1177 (1995).
5. H. Saitoh, T. Tomaru, T. Fujisaki, S. Abe, A. Myojoyama, K. Fukuda, Proceedings of the Tenth EGS4 Users Meeting in Japan, KEK Proceedings, **18**, 55 (2002).
6. B. Casar, U. Zdesar, V. Robar, Radiol. Oncol., **38** (1), 55 (2004).
7. M Allahverdi *et al*, Phys. Med. Biol., **44**, 1125 (1999).
8. A. Nisbet, D. I. Thwaites, Phys. Med. Biol., **43**, 1523 (1998).
9. M. Olivares *et al.*, Med. Phys., **28**, 1727 (2001).
10. G. S. Ding *et al*., Med. Phys., **24**, 161 (1997).
11. M. R. McEwen, A. R. DuSautoy, Phys. Med. Biol., **48**, 1885 (2003).
12. G. S. Ding, D. W. Rogers, T. R. Mackie, Med. Phys., **23**, 361 (1996).
13. D. Mihailescu, C. Borcia, Rom. Rep. Phys., **58** (4), 415 (2006).
14. V. M. Tello *et al*., Med. Phys., **22**, 1177 (1995).
15. International Atomic Energy Agency, *Absorbed dose determination in external beam radiotherapy: An international code of practice for dosimetry based on standards of absorbed dose to water*, Technical Reports series **No. 398**, IAEA, Vienna (2000).
16. International Atomic Energy Agency, The use of plane parallel ionization chambers in high energy electron and photon beams: An international code of practice for dosimetry, Technical Reports series **No. 381**, IAEA, Vienna (1997).
17. America Association of Physicists in Medicine, Task Group 21: *A protocol for the determination of absorbed dose from high energy photon and electron beams*, Med. Phys., **10**, 741 (1983).
18. American Association of Physicists in Medicine, *AAPM's TG 51 protocol for clinical reference dosimetry of high energy photon and electron beams*, Med. Phys., **26**, 1847 (1999).
19. International Commission On Radiation Units And Measurements, *Tissue Substitutes in Radiation Dosimetry and Measurement*, Rep. 44, ICRU, Bethesda, MD (1989).
20. International Commission On Radiation Units And Measurements, *Stopping Powers for Electrons and Positrons*, Rep. 37, ICRU, Bethesda, MD (1984).
21. B. Walters, I. Kawrakow, D. W. O. Rogers, *DOSXYZnrc Users Manual*, National Research Council of Canada Report **PIRS-794** *revB* (Ottawa: NRC).
22. D. W. O. Rogers, I. Kawrakow, J. P. Seuntjens, B. R. B. Walters, E. Mainegra-Hing, *NRC user codes for EGSnrc*, National Research Council of Canada Report **PIRS-702 (revB)** (Ottawa: NRC).
23. I. Kawrakow, D. W. O. Rogers, *The EGSnrc Code System: Monte Carlo Simulation of Electron and Photon Transport*, National Research Council of Canada Report **PIRS-701** (Ottawa: NRC).
24. D. W. O. Rogers, B. Walters, I. Kawrakow, *BEAMnrc Users Manual*, National Research Council of Canada Report **PIRS-0509** (Ottawa: NRC).
25. C.-M. Ma, D. W. O. Rogers, *BEAMDP Users Manual*, National Research Council of Canada Report **PIRS-0509(C)** *revA* (Ottawa: NRC).